

The time-of-flight photocurrent analysis revisited

M. BRINZA^{a*}, G. J. ADRIAENSSENS

Halfgeleiderfysica, University of Leuven, Celestijnenlaan 200D, B-3001 Leuven, Belgium

^aPresent address: Utrecht University, SID – Physics of Devices, P.O. Box 80000, 3508 TA Utrecht, The Netherlands

While the time-of-flight (TOF) photoconductivity experiment was mainly designed to measure the drift mobility and the mobility-lifetime products of both electrons and holes in disordered semiconductors, it has also been used extensively to model the distribution of tail states in the amorphous semiconductors. In general however, such modelling made use of part of the experimental data only, and often relied on crude approximations in its theoretical analysis. Therefore, by using the complete TOF signal, and by matching it to the best available theoretical description of the TOF process, a much better determination of the tail state distributions and other localised states in the gap can now be achieved.

(Received October 16, 2006; accepted November 2, 2006)

Keywords: Time-of-flight photocurrents, Amorphous semiconductors, Density of states, Multiple-trapping transport, Drift mobility, Analytical modelling

1. Introduction

One of the constant challenges in the study of amorphous semiconductors has been the determination of the density and distribution of localised states throughout the band gap of the material. Indeed, while the electronic structure of the bands has been rather well understood – see e.g. Grigorovici et al. [1] – this is not the case for the localised states in the gap. Unfortunately, those states play a dominant role in the conduction processes and a comprehensive knowledge of their characteristics is therefore desirable. Special techniques have been developed to measure the low optical absorption by the localised gap states, and thus the density of states (DOS) in the band gap [2]. However, these techniques – amongst them the Constant Photocurrent Method (CPM), Photothermal Deflection Spectroscopy (PDS), or the recently developed Fourier-Transform Photocurrent Spectroscopy (FTPS) – always result in a joint distribution of conduction and valence band states. Other experimental techniques that aim to elucidate the distribution of gap states, such as Modulated Photoconductivity (MPC) and the Laplace or Fourier transformation of Transient Photocurrents (TPC), are dominated by the majority carriers and thus provide information on just one side of the band gap.

In contrast with the above, the time-of-flight (TOF) transient photoconductivity technique makes it possible to examine the electron and hole components of the current separately and, consequently, is able to offer independent information about the DOS on the conduction and valence band sides of the gap. It is logical, therefore, that results of the TOF experiment have been used to evaluate band tails and defect distributions of amorphous semiconductors, with a strong emphasis on hydrogenated amorphous silicon (a-Si:H), the most applicable one of the group.

In this contribution, we will first provide a brief outline of the basic principles behind the TOF experiment and define the parameters that are used in its interpretation, and then review the early usage of those experimental parameters for DOS modelling. Subsequently, the more recent practice of using the complete TOF signal – rather than just some characteristic parameter – together with an analytic description of the photocurrent transients in order to model DOS will be discussed and illustrated with examples from the current literature.

2. The time-of-flight experiment

The primary aim of the time-of-flight transient photoconductivity experiment is to determine the carrier drift mobility by measuring the time it takes carriers generated at one end of the sample to reach the other end under the influence of a constant electric field. To achieve this goal, the semiconductor to be examined is sandwiched between metallic contacts that form Schottky barriers at the interface, or (as often used in the case of a-Si:H) between doped layers in a p-i-n geometry. At least one of the contacts is made semi-transparent to allow free-carrier generation in the sample by means of a short, strongly absorbed light pulse. A pulsed laser with pulse width near 1 ns is generally used for this. Shortly before the light pulse is triggered, an electric field is applied across the sample such that – depending on the polarity of the field or on the orientation of the p-i-n cell – photo-generated electrons or holes will drift through the sample. A primary photocurrent will be measured in the external circuit due to the charge displacement in the sample, but the potential barriers at the interfaces will block the secondary photocurrents.

Fig. 1 shows some hole transients from a polymorphous Si p-i-n sample, measured at room

temperature with different applied voltages. The vertical lines point to the approximate position of the hole transit time on each curve. Defining such a transit time for the drifting carrier packet is not straightforward due to the high degree of dispersion of the drifting electrons or holes caused by random trapping in the localised gap states. It thus becomes a matter of convention, with the most commonly used definitions being the time at which the current has dropped to half its pre-transit value, or the time at which extrapolations of the pre- and post-transit current slopes intersect. As shown by Seynhaeve *et al.* [3], these conventional definitions correspond more or less to the moment defined by the theoretical concept of the time it would take the mean of the carrier distribution to travel the length L of the actual sample in a semi-infinite model. This definition will be used in the later section dealing with analytical modelling of the transients.

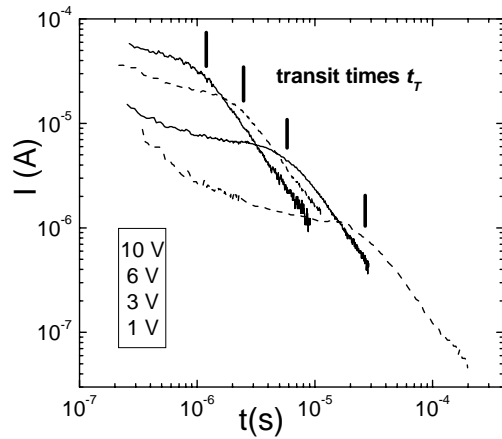


Fig. 1. Room-temperature TOF hole current transients measured on a $3.5 \mu\text{m}$ thick polymorphous silicon (pm-Si:H) sample under application of the indicated voltages. The vertical lines mark the positions of the transit times.

The measured TOF transit time t_T forms the basis for the calculation of the carrier drift mobility, $\mu_d = L/t_T F = L^2/t_T V$, where V represents the applied voltage and F the electric field. It is this quantity μ_d that is mostly quoted when TOF results are reported. An example of a typical diagram of μ_d as a function of the $10^3/T$ for different applied voltages is given in Fig. 2. However, in order for μ_d to be a meaningful quantity, the field F should be, and remain, constant across the sample during the carrier transit. This condition implies that the time between the application of the field and the observation of the carrier transit has to be small with respect to the dielectric relaxation time of the investigated material (on the order of 1 ms for a-Si:H, up to 100 ms for a-Se), and that the photoinjected charge Q_0 must be small with respect to CV , the charge maintained on the sample capacitance C by the applied voltage V .

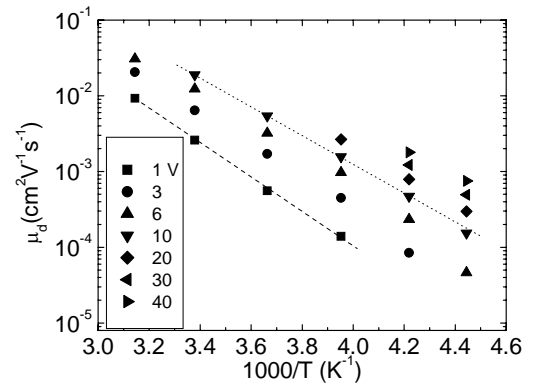


Fig. 2. Measured hole drift mobility vs. inverse temperature as a function of the applied voltage for the same pm-Si:H sample that was used for Fig. 1.

Apart from the transit time, the slopes of the pre- and post-transit currents have often been used to characterise the TOF transients. Those currents can be approximated by power laws according to

$$\begin{aligned} I_{ph}(t) &\propto t^{-(1-\alpha_1)} & , & \quad t < t_T \\ I_{ph}(t) &\propto t^{-(1+\alpha_2)} & , & \quad t > t_T \end{aligned} \quad (1)$$

and the best-fitting values of α_1 and α_2 are taken as experimental data. The fact that the current slopes are negative in both regions is due to carrier trapping into localised states that are located deep enough to prevent re-emission of the charge within the elapsed time. The transport is called (anomalously) dispersive in that case; at higher temperatures non-dispersive transport with a constant initial current, i.e. $\alpha_1 = 1$, can be observed in those cases where the trap distribution is such that the vast majority of trapped carriers have sufficiently short release times $t^* = \nu^{-1} \exp(E^*/kT)$, where ν represents the attempt-to-escape frequency, E^* the particular trap energy, and kT is the Boltzmann energy. The theoretical analysis of TOF transients as shown in Fig. 1 generally makes use of the concept of trap-limited band transport, also called multiple-trapping (MT) transport, whereby carriers remain immobile while trapped and drift in the built-in or applied field only when re-emitted to the transport level [4,5]. Since the average carrier experiences many trapping events into traps of various depths during its transit, the transient current does contain information on the distribution of trapping levels. How this information can be extracted from the data will be the subject of the next sections.

3. Band tail modelling based on resolved drift mobility and current slopes

The MT formalism, as used in the analysis of TOF signals, does encompass a number of simplifying assumptions. The laser pulse is represented by the initial introduction of $Q_0 \delta(t) \delta(x)$ excess free carriers at the transport energy E_0 . These carriers then become trapped with an assumed equal probability into any element of the

localised states distribution $g(E)$. All of these states are considered initially empty and, in view of the TOF requirement $Q_0 \ll CV$ and the high density of localised states in amorphous semiconductors, trap filling can in fact be neglected throughout the MT process. Subsequently, carriers will be released to the E_0 level, and retrapped into gap states at energy E_i according to the release and capture rates

$$r_i = \nu \exp(-E_i/kT) \quad , \quad c_i = g(E_i) \sigma \mu_d F \quad , \quad (2)$$

where σ is the capture cross-section of the traps. The transient photocurrent, proportional to the free carrier density, can in the MT model be written for a discretised energy distribution as [4]

$$I(t) \propto n(t) = A_0 + \sum_{j=1}^N A_j \exp(-s_j t) \quad , \quad (3)$$

where the s_j are the roots of the equation

$$\sum_{i=1}^N \frac{c_i}{r_i - \lambda} = -1 \quad , \quad (4)$$

and the coefficients A_0 and A_j are defined as

$$A_0 = \left(1 + \sum_{i=1}^N \frac{c_i}{r_i} \right)^{-1} \quad , \quad A_j = \left(s_j \sum_{i=1}^N \frac{c_i}{(r_i - s_j)^2} \right)^{-1} \quad . \quad (5)$$

The above expressions follow from the solutions of the Laplace transformed rate equations for the TOF problem [4,6]. Together with the detailed balance relationship from thermal equilibrium that gives

$$\nu = \sigma \mu_d F g(E_0) kT \quad , \quad (6)$$

and the mathematical expression [6]

$$\sum_{j=0}^N \left(t_0 - A_j t - 2 \sum_{k=0, k \neq j}^N \frac{A_k}{s_k - s_j} \right) A_j \exp(-s_j t) = 0 \quad , \quad (7)$$

where t_0 is the trap-free transit time and the solution of which gives the theoretical t_T value described in Section 2, the above equations allow the calculation of μ_d curves of the type shown in Fig. 2 for any proposed DOS.

Application of the above procedure confirmed [7] that the exponential conduction band tail distribution $g(E) = g(0) \exp(-E/kT_0)$ with $T_0 = 312$ K, proposed by Tiedje et al. [8] to model their TOF results on a-Si:H, does indeed reproduce the measured drift mobility data. It was further shown that also for plasma-enhanced chemical vapour deposited (PECVD) a-Si:H samples obtained from Xerox, Palo Alto and SCK/CEN, Mol a similar exponential tail, be it with T_0 closer to 250 K, accounts well for the measured drift mobilities [6]. Nevertheless, other authors have examined analogous μ_d data sets and have, based on different theoretical approximations, come up with different, often more structured tail state distributions.

The basis for these other approaches is often a definition for the transit time as the sum of the trap-free transit time and the time spent on average in the localised states. This time can be written as [3]

$$t_T = t_0 + \sum_{i=1}^N \frac{c_i t_0}{r_i} \quad , \quad (8)$$

whereby the summation is frequently restricted, in practice, to what are deemed to be the most significant terms. Eq. (8) can also be translated in terms of mobilities μ_d and μ_0 with the c_i/r_i ratios expressed in terms of elements of $g(E)$ through a combination of Eqs. (2) and (6). An early application of this type of analysis led Hourd and Spear [9] to conclude that the a-Si:H conduction band tail must drop abruptly some 0.15 eV below the band edge, but an analogous analysis of the same data by Silver et al. [10] concluded that the combination of an initially shallow and then steeper exponential slope was to be preferred. Such double exponential tail state distribution did also follow from the analyses of similar data sets by Longeaud et al. [11] or Nebel and Bauer [12]. Together with the conclusions of Seynhaeve [6] and Tiedje et al. [8] cited above that a simple exponential DOS suffices to model the data, these results strongly suggest that the resolving power of the measured transit times in terms of the underlying DOS is weak. Marshall et al. [13] advocated a still different way of extracting DOS information from the standard $\mu_d(T, F)$ plots by focussing on the relationship between the trapping time of free carriers and the distribution of traps as deduced from the variations in field dependence of the drift mobility activation energy. Again only the measured values of μ_d are involved, which means that of the whole $I(t)$ curve, only the one point in time that defines t_T is taken into consideration. As a consequence, Marshall et al. correctly pointed out that the DOS distribution they proposed only covered the energy range between 0.085 and 0.145 eV below E_C .

Another way of mining the TOF results for DOS information has been to focus on the slopes α_1 and α_2 of the pre- and post-transit currents. Initial analysis [14,15] examined the data in terms of a trial DOS $g(E) = g(0) \exp(-E/kT_0)$, which should result in a unique value for the slopes, $\alpha = \alpha_1 = \alpha_2 = T/T_0$, and in a field dependence of the drift mobility according to

$$\mu_d \propto (L/F)^{-1/\alpha} \quad . \quad (9)$$

This analysis remains valid as long as $\alpha < 1$, *i.e.* for temperatures less than T_0 . In practice however, and certainly for a-Si:H where the analysis was most frequently used, the unique value of α is never obtained from the two slopes at more than one temperature [8,13,16], and the direct proportionality between α and T is poorly obeyed [13,15]. Nevertheless, with α_1 still approximately proportional to T , the analysis in terms of just α_1 remained in use to provide a first-order estimate for the steepness of the band tail. Just like the analysis based on μ_d , the use of α_1 narrows the TOF signal down to one parameter, be it that α_1 takes more of $I(t)$ into account than just the transit time. However, being restricted to shorter times, this analysis can only represent a narrower part of the band tail.

The use of Eq. (9) offers a combination of the μ_d and α_1 data by extracting the $\alpha(T)$ values from $\ln \mu_d$ (or $\ln t_T$) vs. $\ln(L/F)$ plots at various temperatures. It has the further advantage that data from samples with different thickness can be routinely combined into a single diagram. An

example of its use is shown in Fig. 3. A close examination of the results in Fig. 3b reveals that the best straight-line fit through the data would not pass through the origin, and that the ‘resolved’ exponential with $T_0 = 370$ K will hence provide a good approximation to the real valence band tail at best.

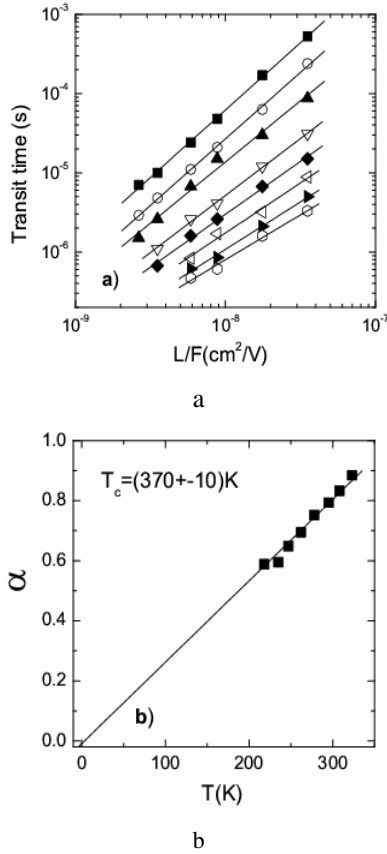


Fig. 3. a) Dependence on the applied field of the hole TOF transit time in a 2.5 μm thick p - i - n sample of PECVD a -Si:H at temperatures between -55 °C and $+50$ °C; b) temperature dependence of the α parameter obtained through the use of Eq. (9) from the data in a). (from M. Brinza [17]).

4. Distribution of deep states from post-transit current analysis

The use of TOF signals to obtain information on the distribution of localised states beyond the band tails is much more straightforward than the above modelling of the tail states themselves. For times $t \gg t_T$, the observed current will be due to the emission of carriers that were trapped in deep states, i.e. well beyond $E_T = kT \ln(\nu t_T)$. Consequently, given the assumption of equal capture cross-section for all localised states, and provided that retrapping into the same deep states is negligible, the post-transit current $I_{pt}(t)$ will at each moment be proportional to the density of states at the energy $E = kT \ln(\nu t)$. Detailed analysis of the situation led to the relationship [18]

$$g(E) = \frac{2g(0)}{Q_0 \nu t_0} I_{pt}(t) \cdot t \quad (10)$$

In order for Eq. (10) to reveal the actual density of gap states, and not just their energy distribution, it will be

necessary to obtain good values for the constants $g(0)$, t_0 , ν and Q_0 . The latter two can sometimes be extracted from the data: Q_0 from an analysis of the collected charge as a function of the applied field, and ν from the temperature dependence of a marked feature in the current decay – if such feature can be resolved. For the parameters $g(0)$ and t_0 on the other hand, estimates on the basis of extrapolations or literature data have to be used. One obstacle in defining an absolute scale for the $g(E)$ distribution is that the constants of Eq. (10) are actually not independent of $g(E)$. This relationship was made explicit through an analysis of the post-transit current by Yan et al. [19], which resulted in the expression

$$I_{pt}(t) \cdot t = \frac{Q_0 kT}{\int_E^{E_F} g(E') dE'} g(E) \quad (11)$$

with E_F referring to the dark Fermi level.

An example of TOF post-transit photocurrents and the DOS profiles that can be derived from them is displayed in Fig. 4. They were obtained with an evaporated a -Se layer [20], and confirm the presence of a defect level some 0.41 eV above the valence band edge. That energy level has been assigned earlier [21] to thermal transitions involving the occupied negatively charged co-ordination defect of a -Se. Given the charged nature of that defect, its capture cross-section will be larger than the one of surrounding neutral localised states; in other words, the DOS in Fig. 4b represents an effective DOS and the maximum seen at 0.41 eV actually represents a maximum of the $\sigma g(E)$ product.

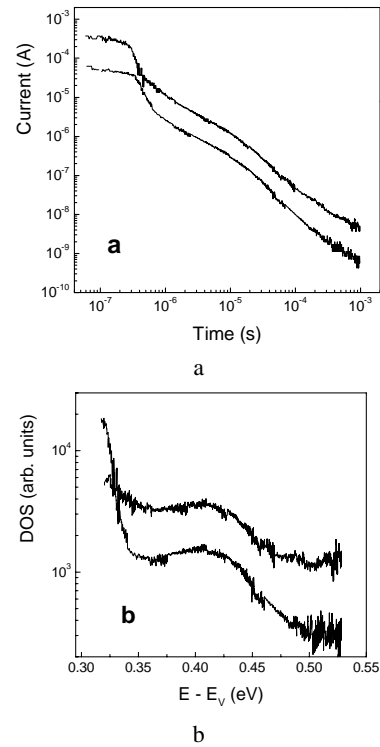


Fig. 4. a) Room-temperature TOF hole transients from 5 μm a -Se sandwich cell with 15 V (upper curve) and 12.5 V (lower curve) applied; b) effective DOS calculated from the data in a) by means of Eq.(10). Curves have been vertically offset for clarity.

5. Modelling of complete current transients

The preceding sections outlined how the slope of the current transient, the functional dependence of the drift mobility on temperature and field, or the post-transit current transients have been used to model the distribution of gap states in the amorphous semiconductors. However, analysis of the TOF results need not be restricted to just those partial results. Since good analytic descriptions of the TOF experiment are available [5,14,22], they can be used to model the actual current transients in the time domain over the range of experimental fields and temperatures. It amounts to using the full information contained in the TOF transients rather than just part of it. As will become evident below from our application of this approach to experimental TOF photocurrents, even details of the tail-state distribution in the region that lies too close to the transport path for easy time-resolved observation, can be readily probed through such modelling.

Although numerical modelling of TOF transients was implemented some time ago on the basis of a discretisation of both the energy and spatial coordinates [6,23], not much use was made of it thereafter. Moreover, with some minor exception [24], that use was restricted to TOF computer modelling that did not encompass the interpretation of experimental data [25]. This state of affairs has recently been altered by the fitting of experimental TOF transients from a variety of a-Si:H samples [26] with calculated curves on the basis of the analytical expressions for the current transients as formulated by Arkhipov and Rudenko [5,22], and by the comparison of experimental a-Se electron TOF transients with the results of optimised Laplace transform solutions for the transients as well as with Monte-Carlo simulations by Koughia et al. [27]. Most frequently a trial DOS that is a combination of a decaying exponential and one or more Gaussian bands is used for the comparison, with the parameters of these components being adjusted until a satisfactory correspondence between experimental and calculated transients is attained. An example of such comparison (from Brinza et al. [26]) is reproduced in Fig. 5. The experimental curves from an a-Si:H sample prepared by the expanding thermal plasma (ETP) method can be modelled with the sum of a decaying exponential with $T_0 = 480$ K and a Gaussian band, centred at $E_V + 0.2$ eV, with a width $\sigma_G = 0.09$ eV. The Gaussian component was needed in this case to duplicate the near coalescence of the post-transit currents at the lower applied fields. Such behaviour differs from the more usual pattern shown in Fig. 1 whereby the post-transit currents for different fields are offset in time, and it then requires a DOS with more structure than a single exponential to model this type of TOF trace.

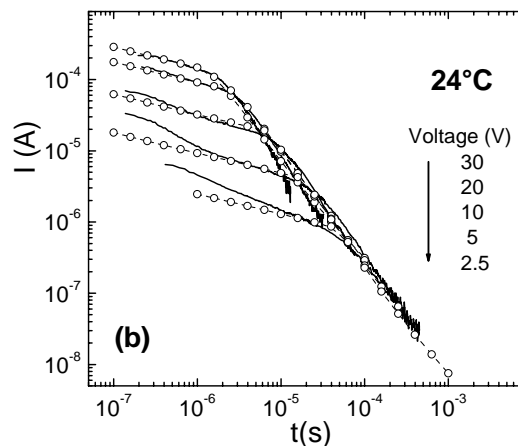


Fig. 5. TOF hole transients from a 5.6 μm thick ETP Cr/a-Si:H/Cr sandwich (full lines) and calculated transients (circles) using a DOS with one exponential and one Gaussian component.

The trial DOS that starts off the optimisation process need not be restricted to elementary exponential or Gaussian functions. Koughia et al. [27] did iterate a spline function with adjustable nodes to match their a-Se TOF signals, but ended up describing their results in terms of one exponential and two Gaussian functions anyway. Procedures for extracting the underlying DOS directly from the measured transient photocurrents have been outlined in the past [28,29], but they invariably lead to involved mathematical formalisms and large uncertainties on the results since the large spread in eigenvalues puts such analysis in the category of ill-posed problems. While it may not be the most elegant way of resolving the DOS to start out with a trial function that reflects the commonly assumed distribution of localized states, it has the advantage of being rather straightforward.

An important experimental requirement for obtaining a dependable image of the real DOS is the use of a sufficiently wide range of TOF data. This point is clearly illustrated by the results obtained by Emelianova et al. [30], and reproduced in Fig. 6. Both parts of Fig. 6 show parts of the same set of TOF transients, measured on an 11 μm thick a-Se sample under various experimental conditions, together with calculated transients that made use for Fig. 6a of the $g(E)$ derived by Koughia et al. [27] on the basis of room-temperature measurements over a limited time range around t_T , while for Fig. 6b the full range of experimental conditions was taken into account in the $g(E)$ optimization. The main difference between the two DOS proposals is lies with the strength and width of a defect band nearly some 0.5 eV below the conduction band; a more prominent and wider band made it possible to model the TOF signals in the millisecond time range as well as for shorter times.

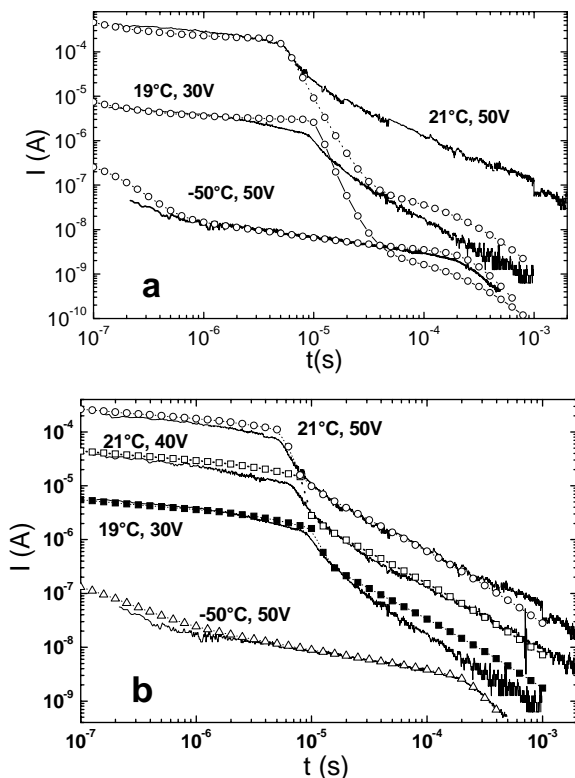


Fig. 6. Electron TOF transients from a-Se sandwich cell (full lines) with a) calculated curves (symbols) based on a DOS proposed in [27] on the basis of a restricted data set, b) calculations based on the full range of experimental data [30]. Individual curves have been vertically offset for clarity.

Once the analytical simulation program for TOF transients has been implemented, it can of course be used equally well for purposes other than the extraction of DOS information. It allowed, for instance, an investigation of the possible link between the Gaussian DOS component that is required to account for the hole TOF transients in ETP a-Si:H samples, and the generally high value of the measured hole mobility in those samples [31]. The study showed that a single Gaussian component can not explain those two independent observations. Another recent use of the analytical modelling concerned the observation of particularly low mobility-lifetime products for electrons in some ETP a-Si:H cells [32]. It could be shown that trapping of electrons in a prominent set of deep traps does explain the observed changes of the TOF transients with measurement conditions as well as the low $\mu\tau$ products.

6. Concluding remarks

Whenever the results of TOF measurements are used beyond their original goal of determining the carrier drift mobility, in which case the aim is generally the modelling of some system parameter, the intrinsic quality of the outcome will be proportional to the reach and diversity of the TOF transients that are taken into consideration. Nevertheless, in interpreting the results of such modelling,

it remains important to remember that all modelling calculations involve some assumptions about basic system parameters. For instance, the free carrier mobility μ_0 that plays a role in TOF calculations can be assumed constant, i.e. independent of electric field and temperature, or it can be given some logical temperature or other functional dependence.

One assumption that is of particular importance for DOS modelling on the basis of TOF results is the widely used one of an energy-independent capture cross-section for all localised states that participate in the multiple-trapping process. This means that a resolved $g(E)$ does in fact represent a $c(E)g'(E)$ product whereby the g' function need not necessarily have the same energy dependence as $g(E)$. In some cases it will be possible to test the equivalence of g and g' when the DOS contains a specific feature that can be independently resolved by another spectroscopic method. The light-induced defects in the gap of a-Si:H constitute one such DOS feature that are placed at the same energy by both post-transit analysis of the TOF signal and optical spectroscopy [19]. Consequently, the energy-independent capture cross-section assumption looks acceptable for the case of a-Si:H.

References

- [1] R. Grigorovici, P. Gartner, I. Corcotoi, J. Non-Cryst. Solids **114**, 256 (1989).
- [2] M. Brinza, M. L. Benkheldir, J. Willekens, E. V. Emelianova, G. J. Adriaenssens, J. Mater. Sci.: Mater. Electron. **16**, 703 (2005).
- [3] G. Seynhaeve, G. J. Adriaenssens, H. Michiel, H. Overhof, Philos. Mag. B **58**, 421 (1988).
- [4] F. W. Schmidlin, Phys. Rev. B **16**, 2362 (1977).
- [5] V. I. Arkhipov, A. I. Rudenko, Philos. Mag. B **45**, 189 (1982).
- [6] G. Seynhaeve, Ph. D. thesis, K.U. Leuven 1989.
- [7] G. J. Adriaenssens, G. Seynhaeve, J. Non-Cryst. Solids **97**, 133 (1987).
- [8] T. Tiedje, J. M. Cebulka, D. L. Morel, B. Abeles, Phys. Rev. Lett. **46**, 1425 (1981).
- [9] A. C. Hourd, W. E. Spear, Philos. Mag. B **51**, L13 (1985).
- [10] M. Silver, E. Snow, D. Adler, J. Appl. Phys. **59**, 3506 (1986).
- [11] C. Longeaud, G. Fournet, R. Vanderhaghen, Phys. Rev. B **38**, 7493 (1988).
- [12] C. E. Nebel, G. H. Bauer, Philos. Mag. B **59**, 463 (1989).
- [13] J. M. Marshall, R. A. Street, M. J. Thompson, Philos. Mag. B **54**, 51 (1986).
- [14] V. I. Arkhipov, M. S. Iovu, A. I. Rudenko, S. D. Shutov, Phys. Stat. Sol. (a) **54**, 67 (1979).
- [15] T. Tiedje in Hydrogenated Amorphous Silicon II, Eds. J. D. Joannopoulos and G. Lucovsky (Springer-Verlag, 1984) p. 261.
- [16] P. B. Kirby, W. Paul, S. Ray, J. Tauc, Solid State Commun. **42**, 533 (1982).
- [17] M. Brinza, Ph. D. thesis, K. U. Leuven 2004.

- [18] G. F. Seynhaeve, R. P. Barclay, G. J. Adriaenssens, J. M. Marshall, *Phys. Rev. B* **39**, 10196 (1989).
- [19] B. Yan, D. Han, G. J. Adriaenssens, *J. Appl. Phys.* **79**, 3597 (1996).
- [20] M. L. Benkhedir, Ph. D. thesis, K. U. Leuven 2006.
- [21] M. L. Benkhedir, M. Brinza, J. Willekens, K. Haenen, M. Daenen, M. Nesladek, G. J. Adriaenssens, *J. Optoelectron. Adv. Mater.* **7**, 2223 (2005).
- [22] A. I. Rudenko, V. I. Arkhipov, *Philos. Mag. B* **45**, 209 (1982).
- [23] C. Main, R. Brüggeman, in *Electronic and Optoelectronic Materials for the 21st Century*, Eds. J. M. Marshall, N. Kirov, A. Vavrek (World Scientific, 1993) p. 270.
- [24] G. Seynhaeve, R. P. Barclay, G. J. Adriaenssens, *J. Non-Cryst. Solids* **97**, 607 (1987).
- [25] R. Brüggeman, C. Main, in *Electronic and Optoelectronic Materials for the 21st Century*, Eds. J. M. Marshall, N. Kirov, A. Vavrek (World Scientific, 1993) p. 279.
- [26] M. Brinza, E. V. Emelianova, G. J. Adriaenssens, *Phys. Rev. B* **71**, 115209 (2005).
- [27] K. Koughia, Z. Shakoor, S. O. Kasap, J. M. Marshall, *J. Appl. Phys.* **97**, 033706 (2005).
- [28] H. Michiel, J. M. Marshall, G. J. Adriaenssens, *Philos. Mag. B* **48**, 187 (1983).
- [29] H. Michiel, G. J. Adriaenssens, *Philos. Mag. B* **51**, 27 (1985).
- [30] E. V. Emelianova, M. L. Benkhedir, M. Brinza, G. J. Adriaenssens, *J. Appl. Phys.* **99**, 083702 (2006).
- [31] M. Brinza, E. V. Emelianova, G. J. Adriaenssens, *Thin Solid Films* **511**, 593 (2006).
- [32] M. Brinza, G. J. Adriaenssens, *Mater. Res. Soc. Symp. Proc.* **910**, A07-04 (2006).

*Corresponding author: M.Brinza@phys.uu.nl